ELSEVIER

Two numerical models for landslide dynamic analysis

Oldrich Hungr*, Scott McDougall[1]

University of British Columbia, Department of Earth and Ocean Sciences, 6339 Stores Road, Vancouver, British Columbia, Canada V6T 1Z4

Abstract

Two microcomputer-based numerical models (Dynamic ANalysis (DAN) and three-dimensional model DAN (DAN3D)) have been developed and extensively used for analysis of landslide runout, specifically for the purposes of practical landslide hazard and risk assessment. The theoretical basis of both models is a system of depth-averaged governing equations derived from the principles of continuum mechanics. Original features developed specifically during this work include: an open rheological kernel; explicit use of tangential strain to determine the tangential stress state within the flowing sheet, which is both more realistic and beneficial to the stability of the model; orientation of principal tangential stresses parallel with the direction of motion; inclusion of the centripetal forces corresponding to the true curvature of the path in the motion direction and; the use of very simple and highly efficient free surface interpolation methods. Both models yield similar results when applied to the same sets of input data.

Both algorithms are designed to work within the semi-empirical framework of the "equivalent fluid" approach. This approach requires selection of material rheology and calibration of input parameters through back-analysis of real events. Although approximate, it facilitates simple and efficient operation while accounting for the most important characteristics of extremely rapid landslides. The two models have been verified against several controlled laboratory experiments with known physical basis. A large number of back-analyses of real landslides of various types have also been carried out. One example is presented. Calibration patterns are emerging, which give a promise of predictive capability.
© 2008 Elsevier Ltd. All rights reserved.

Keywords: Landslides; Mass flows; Avalanches; Runout; Dynamic analysis; Numerical modelling

1. Introduction

A necessary requirement of a quantitative hazard assessment concerned with highly mobile landslides such as debris flows, debris avalanches, flow slides and rock avalanches (cf., Hungr et al., 2001 for classification), is to predict the character and extent of their motion. This is a rapidly developing research field at present. The authors have constructed two microcomputer-based numerical models: a pseudo-three-dimensional Dynamic ANalysis (DAN), Hungr, 1995), based on a depth-averaged, one-dimensional form of the equations of motion and a three-dimensional model DAN (DAN3D) (McDougall and Hungr, 2004, 2005), based on a depth-averaged, two-dimensional form of the same equations. Both models use the simplifying concept

*Corresponding author. Tel.: +1 604 822 8471;
fax: +1 604 822 6088.

E-mail addresses: ohungr@eos.ubc.ca (O. Hungr),
smcdougall@bgcengineering.ca (S. McDougall).

[1]Present affiliation: BGC Engineering Inc., 500-1045 Howe Street, Vancouver, British Columbia, Canada V6Z 2A9.
Tel.: +1 604 684 5900; fax: +1 604 684 5909.

of "equivalent fluid", as described below, and are designed to provide for practical modelling of real landslides, deriving input parameter values from back-analysis of case histories. The objectives are to provide simple solutions that are easy to use, with a minimum number of parameters requiring empirical calibration, but at the same time to account for certain important characteristics of landslide motion, including complex and possibly variable rheology, heterogeneity, internal stiffness and the ability to entrain material from the path (e.g., McDougall and Hungr, 2003).

The purpose of this paper is to present the key features of the algorithms used by DAN and DAN3D.

2. Equivalent fluid concept

Landslides are complex phenomena that are much more difficult to simulate dynamically than fluids because the standard assumptions of hydrostatic, isotropic internal stresses and material homogeneity do not apply. At the same time, the different materials that can be involved may have non-Newtonian rheologies that are strongly influenced by complex interactions during highly unsteady and non-uniform motion across steep and irregular terrain.

Given such complexity, any single material constitutive relationship may only be valid within a narrow domain of space and time. As a result, the traditional scientific approach to analysis, formulating a constitutive law on the basis of fundamental principles and/or laboratory tests and incorporating it into a boundary- or initial-value problem, appears very difficult to apply. Advocates for such a measurement-based approach, including Iverson (1997), Denlinger and Iverson (2001) and Iverson et al. (2004), have demonstrated some success, but so far only in the simulation of controlled experiments.

DAN and DAN3D use a simpler semi-empirical approach based on the concept of "equivalent fluid" (Fig. 1), defined by Hungr (1995) and used tacitly for a long time by many other workers (e.g., Sousa and Voight, 1991; O'Brien et al., 1993; Rickenmann and Koch, 1997). In this framework, the heterogeneous and complex landslide material is modelled as a hypothetical material governed by simple rheological relationships. Internal and basal rheologies may be different from each other. The idea of separation of internal and basal friction mechan-
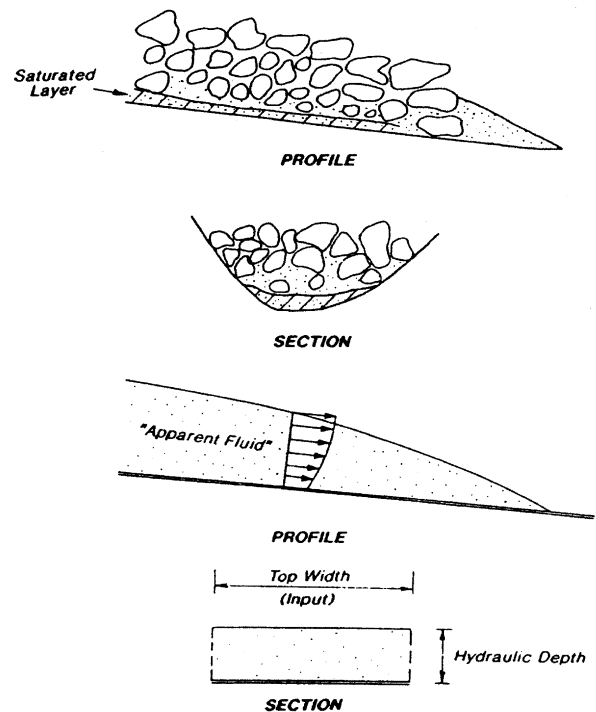

Fig. 1. Schematic illustration of equivalent fluid approach applied to a rock avalanche (after Hungr, 1995). Complex landslide material is modelled as a hypothetical material governed by simple internal and basal rheologies.

isms has its roots in the depth-integrated solutions of classical fluid dynamics, where a variety of viscous or turbulent relationships can be used to determine basal friction forces of a flowing sheet of fluid, while the internal stress distribution is assumed to be hydrostatic (e.g., Chow, 1959). A similar separation was implemented by Savage and Hutter (1989) in what Pudasaini and Hutter (2007) refer to as the SH model. In the original SH model, both the internal deformation and the basal flow resistance are frictional, but with different friction coefficients. This is suitable for modelling flow of sand in smooth-based laboratory flumes, or of natural landslides or avalanches mobilized by a weak, frictional basal layer. Hungr (1995) extended the SH model by replacing the basal friction term by an open rheological kernel, allowing for frictional, viscous or turbulent resistance acting on the base of an internally frictional flow. This corresponds to the situation existing in many natural landslides, where a relatively rigid mass of material flows on top of a much more mobile basal layer. The difference between the properties of the basal layer and the main flowing sheet may be due to differences in

granulometry, porosity and, especially, degree of saturation and pore pressure. There are several common geological mechanisms which are capable of forming such a configuration, as summarized recently by Fell et al. (2007) and Hungr (2007). One more important mechanism is entrainment and liquefaction of saturated material from the path of the flow, described recently by Hungr and Evans (2004).

As in the SH model, the internal rheology is assumed in DAN and DAN3D to be always frictional and is governed by one parameter, the internal friction angle ϕ_i. When ϕ_i equals zero, the model reduces to a standard fluid-dynamics solution with hydrostatic internal stress distribution, as described by Chow (1959) and others. The basal rheological model and its associated parameters, generally only one or two, are selected based on an empirical calibration procedure, in which actual landslides of a given type are subjected to trial-and-error back-analysis. The results are judged in terms of their ability to reproduce the bulk external behaviour of the prototype event, including travel distance and duration and the spatial distribution of velocities and flow/deposit depths (wherever comparable estimates are available from field observations). The calibrated parameters are considered apparent, rather than actual, material properties and cannot, in general, be measured in the laboratory. Extensive back-analysis is required to build a database of input parameters that can be used for prediction for various types of landslides. However, this approach reduces reliance on laboratory-derived material properties and constitutive relationships that may not be valid at full scale. Because the equivalent fluid rheologies are simple and need only a limited number of controlling parameters, the model is easy to constrain. Both velocity and deposit distributions are strongly affected by the chosen rheology. For example, a frictional model produces relatively high velocities and forward-tapering deposits. In contrast, a frictional-turbulent (Voellmy) model predicts lower velocities and deposits that bulge forward (e.g., Hungr and Evans, 1996).

The premise of the equivalent fluid approach is perhaps summarized best by Voight and Pariseau (1978), who wrote, "Any model that allows the slide mass to move from its place of origin to its resting place in the time limits that bound the slide motion is likely to be consistent with the principal observable fact—that of the slide occurrence itself."

In the same sense, continuum dynamic models that can accurately simulate/predict the extent and duration of a landslide and the distribution of intensity (e.g., flow depth and velocity) within the impact area, regardless of the underlying micromechanics, should be considered useful. For the practical purposes of landslide risk assessment, this is the only information that is relevant.

The calibration process should use more than one benchmark event. A common critique of the approach is that, with a sufficiently flexible model, nearly any event can be simulated by choosing a certain set of parameters. What is necessary is to seek patterns of rheological type and parameter ranges that reproduce the behaviour of groups of events of similar description. Predictive capability will result only once such consistent patterns have been identified. This work is now in progress (e.g., Hungr and Evans, 1996; Revellino et al., 2004).

3. The governing equations

The two models are based on Lagrangian forms of the depth-integrated St. Venant equations, applied in curvilinear coordinates, similar to the SH model. Similar governing equations have been derived by a number of workers (e.g., Eulerian forms by: Iverson and Denlinger, 2001; Pastor et al., 2002; Mangeney-Castelnau et al., 2003; Denlinger and Iverson, 2004; Lagrangian forms by: Savage and Hutter, 1989; Gray et al., 1999; Chen and Lee, 2000 and others).

Detailed derivation of the equations behind the DAN3D model can be found in McDougall (2006). It begins from mass and momentum conservation laws governing the mechanics of a continuum:

$$\frac{\partial \rho}{\partial t} + \nabla \cdot \rho \boldsymbol{v} = 0, \tag{1}$$

$$\frac{\partial (\rho \boldsymbol{v})}{\partial t} + \nabla \cdot \rho \boldsymbol{v} \otimes \boldsymbol{v} = -\nabla \cdot \boldsymbol{T} + \rho \boldsymbol{g}, \tag{2}$$

where ρ is the material bulk density, t the time, $\boldsymbol{v}$ the velocity vector, $\boldsymbol{T}$ the stress tensor, $\boldsymbol{g}$ the gravitational acceleration vector, ∇ the gradient operator, $\bullet$ denotes the dot product and $\otimes$ denotes the tensor product.

The equations are developed and simplified in the following steps: The material is assumed to be of constant density and incompressible. This is justified because density variations in granular materials are small in comparison with changes in the other

dynamic variables (for discussion see Savage and Hutter, 1991; Brufau et al., 2000; Denlinger and Iverson, 2004).

The next steps include expanding Eqs. (1) and (2), applying boundary conditions and depth averaging with the use of the Leibniz's rule. The boundary condition applied at the top surface of the flow is zero stress. At the base of the flow, the stress tensor consists of a normal stress corresponding to the hydrostatic gravity potential and a motion-resisting shear stress determined by the appropriate rheological relationship as discussed below.

Material entrainment is accounted for by allowing volume flux across the basal boundary. In physical terms, entrainment consists of direct basal entrainment and frontal plowing. Although plowing is technically a free surface phenomenon, which occurs at the flow front, it is treated here mathematically as a component of basal erosion. The time-dependent rate at which bed material enters the landslide, E, is known as the "erosion velocity" (Takahashi, 1991) and must be positive. A negative erosion velocity in the momentum balance equations would imply, erroneously, that the process is internal to the flow and would produce a thrust in the direction of motion similar to that of a rocket (Erlichson, 1991). In the present version of the model it is assumed that the bulk density of the entrained material is the same as that of the landslide, although this may not always be the case.

The final step is the conversion of the equations to a Lagrangian coordinate system. Both in DAN and DAN3D, the z direction is aligned with the local bed-normal direction and the x direction is aligned with the local direction of motion (Fig. 2). The quantity h is bed-normal flow thickness. The final form of the continuity equation is

$$\frac{\mathrm{D}h}{\mathrm{D}t} + h\left(\frac{\partial(v_x)}{\partial x} + \frac{\partial(v_y)}{\partial y}\right) = E. \quad (3)$$

The Lagrangian forms of the depth-averaged momentum balance equations in x, y and z directions are, respectively (ρ is density, v mean velocity and g are the three components of gravity acceleration):

$$\rho h \frac{\mathrm{D}v_x}{\mathrm{D}t} = -\frac{\partial(\sigma_x h)}{\partial x} - \frac{\partial(\tau_{yx} h)}{\partial y} + \tau_{zx} + \rho h g_x - \rho v_x E, \quad (4)$$
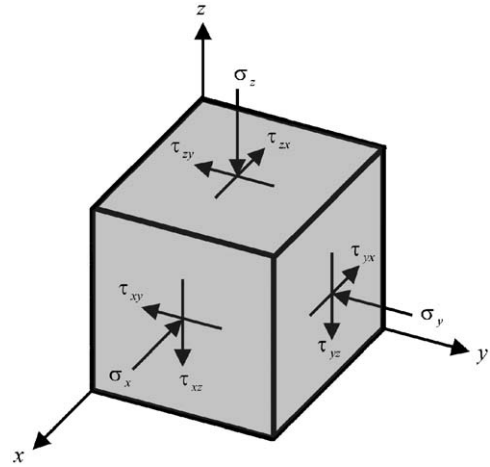

Fig. 2. Total stress state on an element of material within a landslide. Stresses are considered positive as shown. x is direction of motion, z is bed-normal direction.

$$\rho h \frac{\mathrm{D}v_y}{\mathrm{D}t} = -\frac{\partial(\tau_{xy} h)}{\partial x} - \frac{\partial(\sigma_y h)}{\partial y} + \rho h g_y, \quad (5)$$

$$\rho h \frac{\mathrm{D}v_z}{\mathrm{D}t} = -\frac{\partial(\tau_{xz} h)}{\partial x} - \frac{\partial(\tau_{yz} h)}{\partial y} + \sigma_z + \rho h g_z. \quad (6)$$

A Lagrangian approach is useful for two main reasons. First, the convective acceleration terms are eliminated from the momentum balance equations, facilitating subsequent numerical integration and improving efficiency. Second, higher resolution is possible because available computational resources can be concentrated within the simulated slide mass, where they are needed.

Further simplifications can be made using the following scaling argument, which is well-established (cf., Savage and Hutter, 1989; Gray et al., 1999). Assuming that the depth varies gradually and is small relative to the length and width of the landslide, the terms containing shear stress derivatives of τ_{xz} and τ_{yz} in Eq. (6) are small relative to the total bed-normal stress at the base, σ_z and can be neglected. The physical implication of this assumption is that the flow lines must be approximately parallel with the bed. This is the classical shallow flow assumption (e.g., Chow, 1959). Of course, in cases where flow lines are not parallel, certain degrees of approximation emerge.

A further advantage of the Lagrangian framework is that it simplifies the treatment of path curvature, which can be difficult to fully account for in Eulerian models (Mangeney et al., 2007a). Because the instantaneous reference axes are aligned

with the direction of movement, the Lagrangian derivative of v_z is equal to the centripetal acceleration of flow moving along the curving bed in the x direction:

$$\frac{Dv_z}{Dt} = \frac{v_x^2}{R}, \tag{7}$$

where R is the bed-normal radius of curvature of the path in the direction of motion, considered positive for concave curvature. The z direction component of gravity is

$$g_z = -g \cos \alpha, \tag{8}$$

where g is the acceleration due to gravity and α is the inclination of the bed from horizontal.

The above considerations yield the following expression for the total bed-normal stress at the base:

$$\sigma_z = \rho h \left(g \cos \alpha + \frac{v_x^2}{R} \right). \tag{9}$$

Note that the value of σ_z becomes negative when $v_x^2/R > g \cos \alpha$, which implies that the material becomes airborne. Although ballistic/freefall conditions commonly occur in extremely rapid landslides, they are not accounted for explicitly in DAN and DAN3D. As a result, net energy losses associated with impact after freefall must be implicitly accounted for in the basal shear strength term.

Further simplifications are possible with the use of classical soil mechanics techniques (Savage and Hutter, 1989). Assuming that all stresses increase linearly with depth below the free surface, and consistent with Rankine earth pressure theory (e.g., Terzaghi and Peck, 1967), it is useful to normalize the stress state with respect to the total bed-normal stress using pressure coefficients, denoted by k (e.g., $\sigma_x = k_x \sigma_z$ and $\tau_{yx} = k_{yx} \sigma_z$). Normalization of stresses facilitates separate functions in DAN and DAN3D that allow the stress state to be incremented in proportion to the prevailing strain, as detailed in Section 5. Note that the normalization in this case is performed on total stresses, whereas in geotechnics it is performed on effective stresses (i.e., accounting explicitly for pore fluid pressure). The normalized total stress state acting on an element of material within a landslide is shown in Fig. 3.

Finally, it is assumed that spatial variations in the normalized stress state (e.g., $\partial k_x/\partial x$) are relatively small and can therefore be neglected (Gray et al., 1999). Neglecting terms containing derivatives of stress coefficients and rearranging
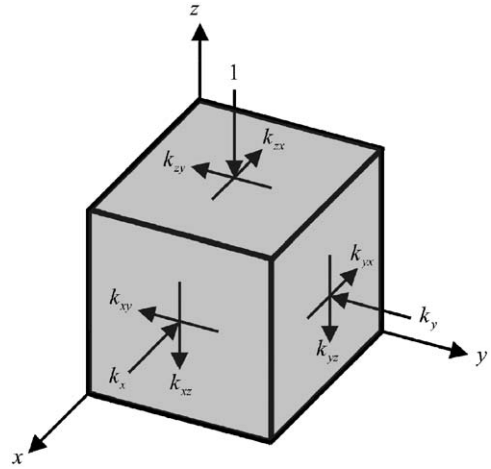

Fig. 3. Normalizing coefficients representing total stress state on an element of material within a landslide. Normalization is with respect to total bed-normal stress (e.g., $k_x = \sigma_x/\sigma_z$). Stress coefficients are considered positive as shown. Compare with Fig. 2.

terms, the Lagrangian forms of the depth-averaged momentum balance equations in the x and y directions are, respectively:

$$\rho h \frac{Dv_x}{Dt} = \rho h g_x - k_x \sigma_z \frac{\partial h}{\partial x} - k_{yx} \sigma_z \frac{\partial h}{\partial y} + \tau_{zx} - \rho v_x E, \tag{10}$$

$$\rho h \frac{Dv_y}{Dt} = \rho h g_y - k_y \sigma_z \frac{\partial h}{\partial y} - k_{xy} \sigma_z \frac{\partial h}{\partial x}. \tag{11}$$

Here, the symbol D/D denotes a Lagrangian differential operator.

It is of interest to note that Eqs. (10) and (11) can be derived phenomenologically, considering the dynamic equilibrium of a reference column: The terms on the left side of Eqs. (10) and (11) are local accelerations of the reference column (multiplied by the mass of the column per unit basal area). The first term on the right side is the gravity force component. The second and third are the "pressure terms", accounting for unbalanced forces resulting from the depth gradient within the flowing fluid. Additional terms appear only in the x direction momentum balance equation due to the assumed orientation of the reference coordinate system parallel with the direction of motion. The fourth term on the right side of Eq. (10) represents the motion-resisting basal shear stress. The fifth term represents momentum flux due to entrainment of path material.

Stresses on the column base are determined by Eq. (9) and by the appropriate rheological relationship. The bed-parallel normal stresses ("pressure terms") are determined based on an assumed stress state within the sliding body. For example, an assumption of the Rankine stress conditions applying to principal stresses yields the Savage-Hutter (1989) equations, discussed below.

This kind of simple phenomenological derivation was used in developing the original model DAN (Hungr, 1995). The ordinary governing equation presented in that paper was derived in such a way. However, it can also be derived from (10) by neglecting transverse shear stresses and lateral (y direction) bed and free surface gradients. Thus, the governing equations are the same in DAN and DAN3D.

Neither model uses the continuity Eq. (3) directly. Instead, each model uses a different type of a Lagrangian surface interpolation algorithm, which satisfies volume conservation implicitly (see below).

4. Basal shear resistance

The basal shear stress, τ_{zx}, opposes motion and, due to the chosen reference coordinate system orientation, is always negative. Consistent with the concept of equivalent fluid, τ_{zx} is governed by a basal rheology that may be different from the internal rheology. To allow the simulation of different types of rapid landslides involving different geological materials, a variety of basal rheological relationships can be implemented in DAN and DAN3D, including laminar, turbulent, plastic, Bingham, frictional and Voellmy rheologies. The user can change the basal rheology along the path or within the slide mass. The equations for τ_{zx} listed below are derived from uniform flow equations corresponding to each given rheology, solving for the basal shear stress as a function of normal flow depth, density, mean flow velocity and rheological parameters.

Laminar flow may be useful for approximate analysis of certain fully liquefied flows involving granular or clayey materials. In the DAN3D coordinate system (μ is the dynamic viscosity):

$$\tau_{zx} = -\frac{3\mu v_x}{h}. \tag{12}$$

Turbulent flow of water or granular mixtures with low solids concentration are routinely analysed in engineering applications using the Manning equation (n is the Manning coefficient):

$$\tau_{zx} = -\frac{\rho g n^2 v_x^2}{h^{1/3}}. \tag{13}$$

A common alternative to Eq. (13) is the Chézy equation:

$$\tau_{zx} = -\frac{\rho g v_x^2}{C^2}, \tag{14}$$

where C is the Chézy coefficient, which is related to Manning's n by $C = h^{1/6}/n$.

Plastic flow is often assumed in geotechnical engineering analyses related to pseudo-static motion of liquefied soil, when the basal shear resistance is assumed to be equal to a constant yield strength:

$$\tau_{zx} = -c. \tag{15}$$

The *Bingham resistance model* combines plastic and viscous behaviour. A Bingham fluid behaves as a rigid material below a threshold yield strength, but as a viscous material above. The following cubic equation must be solved to determine the basal shear resistance (its derivation uses the same approach as mentioned above):

$$\tau_{zx}^3 + 3\left(\frac{\tau_{yield}}{2} + \frac{\mu_{Bingham}v_x}{h}\right)\tau_{zx}^2 - \frac{\tau_{yield}^3}{2} = 0, \tag{16}$$

where τ_{yield} is the Bingham yield stress and $\mu_{Bingham}$ is the Bingham viscosity.

Frictional basal resistance is proportional to the effective bed-normal stress at the base, σ_z', which is the difference between the total stress, σ_z, and the pore fluid pressure at the base, u:

$$\tau_{zx} = -(\sigma_z - u)\tan\phi = -\sigma_z'\tan\phi, \tag{17}$$

where ϕ is the dynamic basal friction angle. Pore fluid pressure within a moving landslide is extremely difficult to estimate, as it is strongly dynamically coupled to the changing level of total normal stress in the material, while at the same time subject to time-dependent diffusion. In geotechnical slope stability analysis, it is commonly assumed that the pore pressure is related to the total stress by a pore-pressure ratio, $r_u = u/\sigma_z$, in which case:

$$\tau_{zx} = -\sigma_z(1 - r_u)\tan\phi. \tag{18}$$

If r_u can be assumed constant, the basal stress relationship remains frictional (i.e., the total normal stress and shear stress remain proportional). Eq. (17) can then be simplified to include only one independent variable, a bulk basal friction angle ϕ_b,
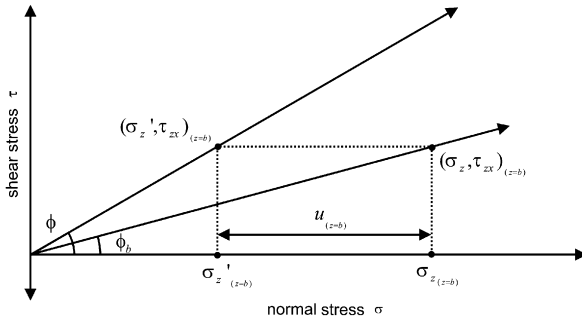
Fig. 4. Relationships between frictional parameters in Eqs. (18) and (19).

where $\tan \phi_b = (1 - r_u) \tan \phi$:

$$\tau_{zx} = -\sigma_z \tan \phi_b. \tag{19}$$

Use of a constant pore-pressure ratio or bulk basal friction angle assumes loading response that is intermediate between purely drained and undrained responses. It is an approximation that needs to be validated as part of the calibration process. The relationships between the various frictional parameters are shown in Fig. 4.

The *Voellmy resistance model* combines frictional and turbulent behaviour:

$$\tau_{zx} = -\left(\sigma_z f + \frac{\rho g v_x^2}{\xi} \right), \tag{20}$$

where f is the friction coefficient and ξ is the so-called turbulence parameter. The first term on the right side accounts for any frictional component of resistance and has the same form as Eq. (17) (f is analogous to $\tan \phi_b$). The second term was originally introduced by Voellmy (1955) to account for the velocity-dependent influence of air drag on snow avalanches and has the same form as Eq. (14) (ξ is the square of the Chézy coefficient). In the context of landslide dynamics and the equivalent fluid approach, the second term is not included to account for either air drag or turbulence alone, but rather to empirically account for all possible sources of velocity-dependent resistance (additional to the effects of path curvature and momentum transfer during entrainment, which are accounted for explicitly in both DAN and DAN3D). The Voellmy rheology has been used successfully by many researchers to model various types of mass movements, including snow avalanches, rock avalanches, flow slides, debris avalanches and debris flows (e.g., Perla et al., 1980; Körner, 1976; Hungr

et al., 2002; Revellino et al., 2004; Rickenmann and Koch, 1997).

5. The pressure terms

As mentioned above, the pressure terms in Eqs. (10) and (11) depend on assumptions regarding the tangential (bed-parallel) stress state in the flowing sheet. In a fluid, of course, these are simply hydrostatic stresses, i.e., zero shear and a constant, hydrostatic normal stress. In Eqs. (10) and (11), this condition would result in both k_{zx} and k_{zy} being zero, while $k_x = k_y = 1.0$. In a flowing, deforming sheet of frictional material, on the other hand, the k coefficients are functions of longitudinal strain. Savage and Hutter (1989) derived a formula for k_x and k_y, based on the assumption that the material is at the point of shear failure, controlled by an internal friction angle φ_i and a basal friction given by the ratio of basal shear stress to the total normal stress ("the friction slope", k_{zx}):

$$k_{x(\min/\max)} = 2 \left(\frac{1 \pm \sqrt{1 - \cos^2 \phi_i (1 + k_{zx}^2)}}{\cos^2 \phi_i} \right) - 1. \tag{21}$$

The minimum and maximum values of the coefficient depend on the sense of internal shearing. Under the "active" condition, when the flowing sheet is stretching, the minimum value applies. The maximum value corresponds to the "passive" condition, when the sheet is being compressed. In both DAN and DAN3D, the stress states are determined by tangential strain. At the onset of motion, k_x is taken as 1.0, corresponding to a hydrostatic "at rest" condition. From that point on, both numerical codes keep a record of the developing strain at each reference column. Transition from active to passive condition occurs in both programs by incrementing the k-coefficients through multiplication of strain increments by a stiffness coefficient, D:

$$k = k' + D \Delta \varepsilon, \tag{22}$$

where the primed value of k applies at the beginning of a time step, $\Delta \varepsilon$ is the strain increment occurring during the time step and D is a dimensionless stiffness coefficient, which is assumed to be spatially and temporally constant (strain is considered positive under compression). The current default value in DAN3D is 200 for both compression and extension. This is within the range of dimensionless

stiffness coefficients estimated by Hungr (1995), which were based on measured values of stiffness of granular soil behind retaining walls during active and passive deformation (Terzaghi and Peck, 1967). The results show that neither DAN nor DAN3D is sensitive to the specified value of D, but certain smaller values can substantially aid numerical stability. With this approach, stress response occurs over several time steps, smoothing anomalous strain interpolations and preventing numerical oscillation between active and passive stress states. This may be one reason why neither model requires numerical damping. With the exception of Denlinger and Iverson (2004), other existing models assume instantaneous stress response, equivalent to using an infinite value.

It must be noted here that Savage and Hutter's Eq. (21) is an approximation, valid strictly only under the condition of simple shear, existing when the flow lines are parallel (i.e., under uniform flow). However, its underlying assumption of fully mobilized internal shearing is not compatible with uniform flow. Thus, the approximation inherent in these equations adds to the error connected with the shallowness assumption in general and this makes the method perform rather poorly in cases involving substantial bed-normal velocities, such as the dam-break solution. This is a subject of current investigation by the authors. Also, the equation is incorrect when the internal and basal friction angles are of similar value, yielding a k value greater than 1.0. Physically, the planes of general internal shearing become parallel with the bed. However, there is no reason for general shear failure to occur on these planes, as any surface within the flowing mass is as liable to fail as any other. Nevertheless, the equation has performed well in a number of test cases and must be accepted, for now, as a reasonable approximation, at least for shallow flows.

Another assumption applied in the current version of DAN3D is that the tangential normal stresses are the principal stresses in the direction x, i.e., in the direction of motion. As a result, k_{yx} and k_{xy} in Eqs. (10) and (11) are zero. It is useful to compare this assumption with those used by other workers. Gray et al. (1999) assumed that the principal axes correspond with the mean downslope direction. When the mean downslope direction equals the actual downslope direction and the direction of motion is exactly downslope, the assumptions used in DAN3D and by Gray et al. (1999) are identical. In contrast, Chen and Lee (2000) assumed that the principal axes are

aligned with a global coordinate system, which makes the results dependent on the choice of global coordinate orientation. Similarly, Iverson and Denlinger (2001) assumed that the principal axes are oriented at a fixed angle from arbitrarily oriented local coordinate axes. The DAN3D assumption that the principal axes are aligned with the direction of motion is by no means exact, especially in the case of strongly curving flow or flow around obstacles, but one that appears the most intuitive of those mentioned above.

The numerical scheme also makes a check on internal yield between k_x and k_y. Details are described in McDougall (2006).

6. Free surface interpolation

The continuity equation (3) is not directly used in either DAN or DAN3D. Instead, continuity is implicit through the use of control volumes, attached to the reference columns. In DAN (Hungr, 1995), the control volumes are trapezoidal "mass blocks" representing the material carried between each adjacent pair of reference columns. The flow thickness in the centre of each mass block and each reference column are established after each time step by linear interpolation. The model allows the mass blocks to change width according to a user-prescribed width function, thus taking account of lateral spreading or narrowing of the flowing mass in terms of volumetric continuity. It must be noted that DAN neglects momentum losses resulting from lateral width changes. This is an approximation analogous to the shallowness assumption. Comparisons between this "pseudo-3D" solution and DAN3D, which takes lateral momentum conservation into account have so far been favourable, as mentioned later in this paper.

DAN3D, on the other hand, is based on Smoothed Particle Hydrodynamics (e.g., Wang and Shen, 1999). The method has earlier been used for avalanche dynamics by Laigle and Coussot (1997) and others. Its implementation in DAN3D is simple. A bell-shaped control volume, described by a Gaussian function kernel is attached to each reference column. The flow surface and its inclinations at any given point after each time step is re-established by adding the thickness and gradient of all control volumes within a radius of influence (see Fig. 5). The control volumes remain constant, assuring volumetric continuity, unless purposely enlarged by entrainment. The SPH interpolation is
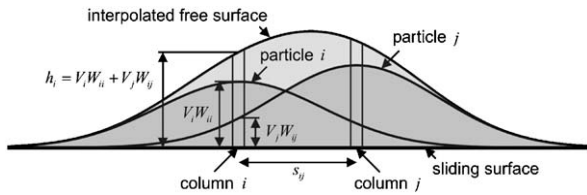
Fig. 5. A physical interpretation of SPH in a depth-averaged framework. When interpolating kernel is Gaussian, particles can be visualized as bell-shaped objects. Total depth and depth gradient at any location are determined by superposition of particles.

not fully shock-capturing, but it does smooth out less intensive shocks.

7. Material entrainment

Material entrainment depends on slope, flow velocity, strength and quantity of the basal material available for entrainment. Entrainment may occur at the front by "ploughing", or beneath the body of the flowing mass as step or basal erosion (Sovilla et al., 2006). Some algorithms that predict the entrainment rate from descriptive parameters have been proposed in the literature for dry granular material (Mangeney et al., 2007b) and layered snow (Sovilla et al., 2006). However, a similar algorithm for entrainment of saturated soil is likely very complex, as a result of dramatic weakening of the soil caused by undrained pore-pressure response to rapid loading. A simple model of material entrainment was incorporated in DAN in its original version (Hungr, 1995). In DAN, the erosion rate increases in proportion to the flow depth, resulting in a depth-proportional distribution of entrained material and natural exponential growth of the landslide with displacement. The erosion amount is limited by a user-defined, spatially distributed "erosion depth". The rate of entrainment is dimensioned in DAN so that the full erosion depth is reached at any point of the path within the user-specified entrainment zone, once the entire current moving volume of the slide has crossed that point. This assumption stresses step entrainment and basal erosion mechanisms and neglects plowing as defined by Sovilla et al. (2006). This is probably appropriate for dealing with saturated soil, where undrained loading is the major mobilization mechanism (Sassa, 1985). DAN3D uses a similar empirical approach based on a user-prescribed parameter, E (the erosion velocity), which represents the bed-normal depth

eroded per unit flow depth and unit displacement or, equivalently, the displacement-dependent natural exponential growth rate (McDougall and Hungr, 2005). This method has a physical basis, as the changes in stress conditions leading to failure within the path material can be related to the flow depth. In contrast, in the formulation of Chen et al. (2006), the erosion rate is independent of the flow depth. The difference between these two formulations must be resolved by comparisons with field-observed behaviour. High values of E can presumably be used to simulate ploughing mechanisms, although no research on this has been completed to date.

In both DAN and DAN3D, the amount of material entrained from points along the path in each time step is added to the nearest control volume. The entrainment amount is limited by a user-defined erosion depth, specified within a prescribed entrainment zone. Neither model presently modifies the path as a result of material erosion.

The assumption of natural exponential growth with displacement is used for its simplicity and may eventually serve as a baseline for more complex entrainment modelling, including the development of constitutive relationships for growth rates that are based on actual entrainment mechanisms. Similar to the open basal rheological kernel used in DAN3D, the user could potentially select an appropriate entrainment relationship from a menu of proposed models. Such models could incorporate dependence on other factors, including flow velocity, slope angle, path curvature, surface roughness or the strength and drainage characteristics of local path material. In the meantime, different values of E and erosion depth can be assigned to distinct entrainment zones to empirically account for such factors.

8. Strain interpolation

As described in Section 5, both DAN and DAN3D use actual values of tangential (bed-parallel) strain to assign values to the earth pressure (k) coefficients of Eq. (21). In DAN, the strain is recorded directly as a function of increasing or decreasing tangential distance between adjacent pairs of reference columns. The k coefficients are initialized to the hydrostatic value of 1.0. Then, as the flowing sheet contracts or expands depending on the shape of the path, the k-coefficient is increased or decreased based on incremental stress changes and an assumed stiffness coefficient, according to
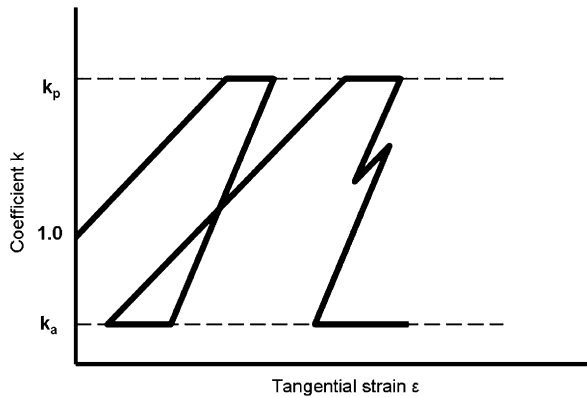
Fig. 6. Development of tangential pressure coefficient (k_x or k_y) with changing cumulative tangential strain. Slopes of curve represent stiffness D. In DAN, a different stiffness is used on loading and unloading. In DAN3D they are the same (after Hungr, 1995).
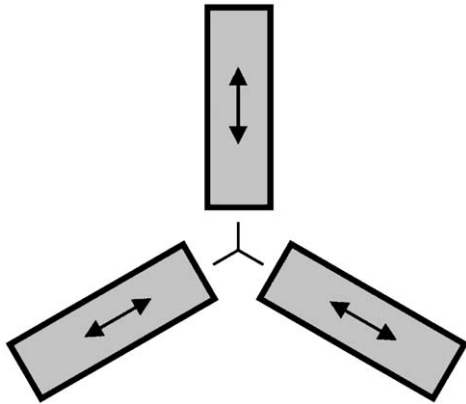

Fig. 7. Plane strain measurement using strain gauge rosettes, a common technique in structural and mechanical engineering. Complete plane strain state (e.g., in a flat metal plate) can be determined using only three directional strain measurements. Directions can be arbitrary, as long as they are different.

Eq. (22). Of course, the increase or decrease is limited by the full value of the "passive" or "active" values calculated by Eq. (21) (see Fig. 6).

Strain determination is more complicated in 3D. The particle-tracking nature of the SPH method provides a framework for approximating the incremental tangential strain state at each reference column location. Tangential flow deformation can be approximated from relative particle motion; converging particles indicate flow compression while diverging particles indicate flow extension. DAN3D uses an approach analogous to strain measurement in flat plates using strain gauge rosettes (Fig. 7).
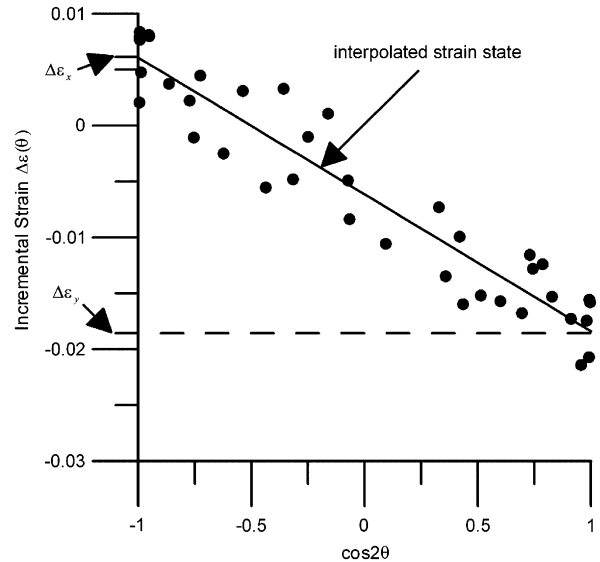

Fig. 8. Example of a DAN3D incremental tangential strain interpolation using simplified method. Relative positions of neighbouring particles are updated at each time step and strain increments are calculated for each neighbouring particle. A least-squares fit of linear equation (23) provides an estimate of column/particle-centred strain state.

After some testing of other, more complex assumptions, the method was again simplified by assuming that the principal strain occurs in the direction of motion. Assuming that $\Delta\varepsilon_x$ (in the direction of motion) and $\Delta\varepsilon_y$ approximate the principal incremental tangential strains and using conventional strain compatibility theory, the particle-centred incremental tangential strain state at a point becomes

$$\Delta\varepsilon(\theta) = \left(\frac{\Delta\varepsilon_x + \Delta\varepsilon_y}{2} + \frac{\Delta\varepsilon_x - \Delta\varepsilon_y}{2} \right) \cos 2\theta, \qquad (23)$$

where θ is a parametric angle in the local x-plane, measured counter-clockwise from the positive yx-axis.

This approach is analogous to strain measurement using a two-gauge rosette, in which the gauges are aligned with the assumed directions of the principal strains. Eq. (23) has the form of a straight line. Similar to the two-gauge rosette method, when exactly two neighbouring particles are present there are two equations and the system is determined. With less than two neighbours the system is indeterminate and the influence of strain must be neglected. With more than two neighbours, the system is redundant and a two-parameter least-squares approximation is used to fit a line to the

data points, providing estimates of $\Delta\varepsilon_x$ and $\Delta\varepsilon_y$. An example is shown in Fig. 8.

9. Numerical implementation

The DAN model is coded in Visual Basic and runs on standard microcomputers, requiring input in the form of a path profile, central thickness of the source volume and the flow width function. The path profile is smoothed by fitting a spline function. An individual analysis lasts less than 1 min.

The DAN3D model has been coded in C++ and runs on an IBM-compatible personal computer. The programme reads spatial data in the form of user-created grid files, which contain the following data at nodal locations on a global fixed grid: (1) the bed elevation; (2) the landslide source depth (the distance between the original ground surface and the rupture surface, measured in the vertical direction and increased as appropriate to account for dilation/bulking of the failed mass); and (3) the depth of the erodible bed (measured in the bed-normal direction). A moderate amount of smoothing of the path digital elevation model (DEM) is usually required. The surface details that are lost in the process must be accounted for implicitly in the basal shear stress term. The user inputs the required rheological and control parameters, such as the time step interval. A variety of data files can be output at user-prescribed intervals and processed by a 3D surface-modelling programme, such as Surfer (Golden Software Inc.) or a suitable GIS package. The final output takes the form of velocity or depth contour maps and static or animated isometric views.

The duration of each simulation depends on the number of particles used, the size of the global reference grid, the length of the time step interval, the frequency of output required and the nature of the landslide in question. For a typical simulation using 4000 particles, a 2 GHz computer processes approximately one time step per second and the duration of a typical analysis is about 30 min.

10. Verification testing

Verification of models of this type usually requires the analysis of controlled laboratory experiments, in which the rheological kernel as well as the controlling parameters are independently known, or comparison with other, independently developed models. The DAN model was verified by analysing several laboratory experiments involving dry sand flow over smooth base, a laboratory flume experiment involving laminar flow of oil of known viscosity and comparisons with other model results (Hungr, 1995). DAN3D was verified using straight dry sand flow experiment carried out by Gray et al. (1999) and deflected flow experiments carried out by the authors at the University of British Columbia (McDougall and Hungr, 2004, see also Pudasaini and Hutter, 2007). The letter tests, in particular, demonstrated the ability of the model to "steer" the flow around topographic obstructions. Both models have been verified for the hydrostatic case using analytical dam break solutions (e.g., Stoker, 1957; Mangeney et al., 2000). Other verification testing is described by McDougall (2006).

11. Example result

The use of the 2D model DAN and its 3D counterpart DAN3D is illustrated by the example of a rock avalanche from the Swiss Alps. On May 30, 1946, a magnitude 4.4 earthquake triggered a rock avalanche in the Andins Valley in Valais, Switzerland (CREALP, 2001). The event initiated as a slide in limestone on the south face of an eastern arête of Six des Eaux Froides. Normal faults dipping at about 40–43° to the south formed the main failure surface between elevations 2300 and 2700 m (CREALP, 2001).

The slide mass overrode talus on the source slope and impacted Lake Luchet and its surrounding marshy areas on the valley floor. Rapid undrained loading (e.g., Sassa, 1985) and entrainment of this wet and weaker path material probably contributed to the relatively high mobility of the event, which had a fahrböschung of only 16° (CREALP, 2001).

A ridge in the valley, oriented perpendicular to the initial direction of motion, deflected the flow both westward (up-valley) and eastward (down-valley). The eastern distal flow travelled about 1.5 km from the toe of the source slope and formed a relatively shallow, muddy deposit (CREALP, 2001). Secondary rock falls and slides may have contributed to the deeper and coarser proximal deposit, although the timing and total duration of the event are unknown (CREALP, 2001). An oblique aerial view of the landslide area is shown in Fig. 9.

Pre and post-event DEMs were provided. The source depths were approximated by subtracting the post- from the pre-event DEM. The resulting source

Fig. 9. Oblique aerial view of Six des Eaux Froides rock avalanche (looking northwest). Photograph courtesy of Raphaël Mayoraz.
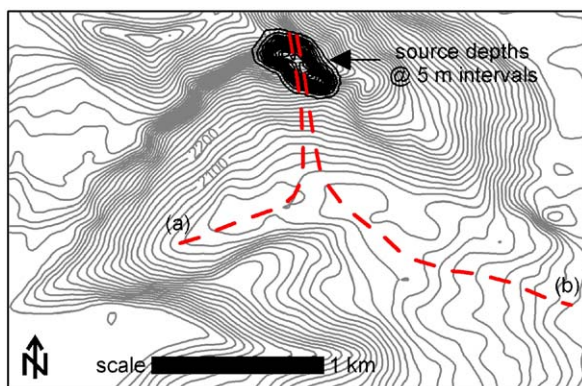

Fig. 10. Initial conditions, showing two path streamlines used in DAN back-analyses (a) and (b). Source depths are at 5 m intervals and sliding surface elevations are at 20 m intervals.

volume of approximately $4.2\,M\,m^3$ was bulked 20% to account for fragmentation, giving a total slide volume of approximately $5\,M\,m^3$. The initial conditions are shown in Fig. 10.

The event was back-analyzed first using the 2D model DAN. To simulate the division of flow up and down the valley, two separate analyses were performed along path profiles corresponding to the two main streamlines of motion, denoted by (a) and (b) in Fig. 10. In similar proportion to the real event, slide volumes of 2 and $3\,M\,m^3$ were used in cases (a) and (b), respectively. Path widths in each case were estimated from post-event aerial photographs.

The Voellmy resistance model shown in Eq. (20) was used. The two Voellmy parameters were systematically adjusted until both simulations approximately reproduced the observed: (1) total travel distance and (2) distribution of deposits. Better constraint of the input variables would have been possible with independent flow duration and velocity estimates, but none were available. Nevertheless, the need to satisfy the above two calibration criteria in both cases provided reasonably tight constraint.

A DAN3D simulation using the entire $5\,M\,m^3$ slide volume and the same calibrated Voellmy parameters was then performed. In both the DAN and DAN3D cases, an internal friction angle of $35°$ was used to limit the internal stresses. This value is considered appropriate for the dry, granular rock avalanche material that comprised the bulk of the main mass, although neither model is very sensitive to this parameter within a reasonable range (for this type of a problem). Volume changes due to entrainment, which were likely small relative to the source volume in this case, were neglected.

The results of the two DAN analyses are shown in Fig. 11. The best simulations of the total travel distance and distribution of deposits in cases (a) and (b) were obtained using a friction coefficient of $f = 0.13$ and a turbulence parameter of $\xi = 450\,m/s^2$. These values are close to the values of $f = 0.1$ and $\xi = 500\,m/s^2$ recommended by Hungr
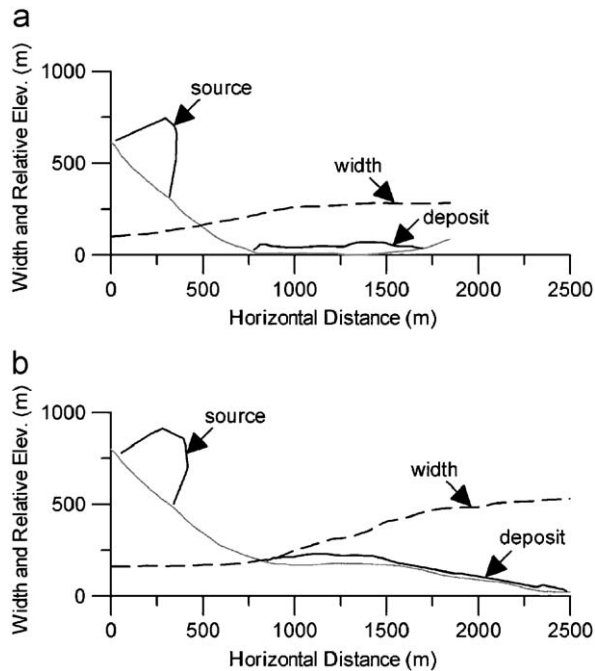
Fig. 11. Results of two DAN analyses using Voellmy parameters $f = 0.13$ and $\xi = 450 \, \text{m/s}^2$: (a) up-valley and (b) down-valley. Source and deposit depth profiles are exaggerated $5 \times$ for clarity. Total duration of case (b) was approximately 150 s.
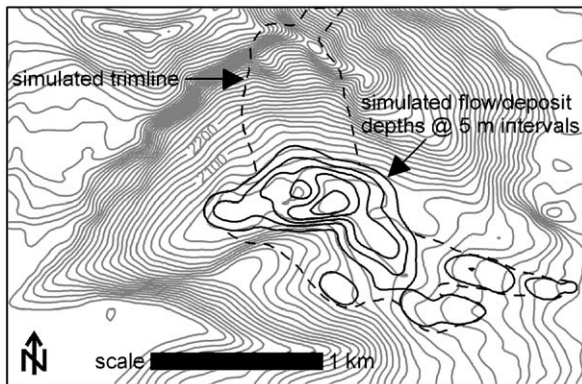

Fig. 12. Results of DAN3D analysis using Voellmy parameters $f = 0.13$ and $\xi = 450 \, \text{m/s}^2$ after 150 s. Simulated flow/deposit depths are at 5 m intervals and sliding surface elevations are at 20 m intervals.

and Evans (1996) on the basis of DAN back-analyses of 23 other rock avalanches. In case (b), the main proximal deposit and the long and relatively thin distal deposit were reproduced, in approximately the same proportion as estimated by CREALP (2001). The total duration of case (b) was just over 150 s, with frontal velocities up to 87 m/s recorded near the toe of the source slope.

Both of these values are within reason for a long-runout rock avalanche of this size.

The results of the preliminary DAN3D simulation using the same input parameters ($f = 0.13$ and $\xi = 450 \, \text{m/s}^2$) are shown in Fig. 12. Good correspondence between these results, the real event and the preceding DAN results is evident. DAN3D correctly reproduced the relatively thick proximal deposits and division of flow caused by the ridge in the valley. In the subsequent down-valley, distal flow was also simulated, although it did not come completely to rest within 150 s (the flow front was still moving at about 8 m/s at this time). The reason for this is that the slope gradients in the distal path remained higher than the specified friction coefficient, in contrast to the flatter distal path used in DAN case (b), which did not follow the direction of steepest descent. This sensitivity to slope gradient is an important characteristic of the Voellmy model and other basal resistance relationships that include a frictional term.

The simulated runup against the ridge was also too high (some overtopping occurred, which was not observed in the real event). This could have been caused by necessary smoothing of topographic details in the DEM, that may have reduced the steepness of the ridge. Despite these small discrepancies, both models provided very good approximation of the observed behaviour. Notably, both models provided very similar results in terms of total runout distances both in up-valley and down-valley directions, as well as flow thicknesses and velocities. This correspondence is typical when DAN and DAN3D are run with the same data (including the width function which must, however, be input by the user in the case of DAN).

In practice, significant efficiency can be gained by taking advantage of the correspondence between the two models and using them together in a complementary manner. Preliminary input parameters can be selected from the existing database of calibrated values. DAN3D can then be used to estimate the path direction and width, and DAN can in turn be used to rapidly adjust the resistance parameters. This added efficiency is equally important for trial-and-error back-analysis and parametric forward analysis, both of which require multiple model runs.

12. Conclusion

The two models represent versatile tools for simple, albeit somewhat approximate, DAN of

rapidly moving landslides of various types. DAN and DAN3D are based on the same theory, use similar numerical solution methods and produce similar results when applied to similar data. The system of governing equations used in DAN and DAN3D has been derived from first principles both mathematically and phenomenologically using a straightforward series of explicit and justifiable assumptions and approximations. The generality of the system, in accordance with the equivalent fluid approach, makes it applicable in a wide variety of situations. This flexibility facilitates the simulation of real landslides within the constraints of practical landslide hazard and risk assessment. An example is presented illustrating the use of the two models.

Numerous other examples of real landslides have now been back-analysed with the two models and patterns of typical rheologies and resistance parameters are beginning to emerge, with a prospect of predictive capability (e.g., Hungr et al., 2005).

Acknowledgements

References

Brufau, P., Garcia-Navarro, P., Ghilardi, P., Natale, L., Savi, F., 2000. 1D mathematical modelling of debris flow. Journal of Hydraulic Research 38, 435–446.

Chen, H., Lee, C.F., 2000. Numerical simulation of debris flows. Canadian Geotechnical Journal 37, 146–160.

Chen, H., Crosta, G.B., Lee, C.F., 2006. Erosional effects on runout of fast landslides, debris flows and avalanches: a numerical investigation. Geotechnique 56, 305–322.

Chow, V.T., 1959. Open-Channel Hydraulics. McGraw-Hill, New York, NY, 680pp.

CREALP, 2001. Éboulement du 30 Mai, 1945 du Six des Eaux Froides près du Rawyl (Valais). (Rockslide of May 30, 1945 at Six des Eaux Froides near Rawyl, Valais). Centre de Recherche sur L'Environnement Alpin, Sion, Switzerland (report in French, 50pp).

Denlinger, R.P., Iverson, R.M., 2001. Flow of variably fluidized granular masses across three-dimensional terrain, 2. Numer-ical predictions and experimental tests. Journal of Geophy-sical Research 106 (B1), 553–566.

Denlinger, R.P., Iverson, R.M., 2004. Granular avalanches across irregular three-dimensional terrain: 1. Theory and computation. Journal of Geophysical Research 109, F01014.

Erlichson, H., 1991. A mass-change model for the estimation of debris-flow runout: a second discussion: conditions for the application of the rocket equation. Journal of Geology 99, 633–634.

Fell, R., Glastonbury, J., Hunter, G., 2007. Rapid landslides, the importance of understanding mechanisms and rupture surface mechanics, 8th Glossop Lecture. Quarterly Journal of Engineering Geology and Hydrogeology 40, 9–27.

Gray, J.M.N.T., Wieland, M., Hutter, K., 1999. Gravity-driven free surface flow of granular avalanches over complex basal topography. Proceedings of the Royal Society of London, A 455, 1841–1874.

Hungr, O., 1995. A model for the runout analysis of rapid flow slides, debris flows, and avalanches. Canadian Geotechnical Journal 32, 610–623.

Hungr, O., 2007. Dynamics of rapid landslides. In: Sassa, K., Fukuoka, H., Wang, F., Wang, G. (Eds.), Progress of Landslide Science. Springer Verlag, Heidelberg, Germany, pp. 47–57.

Hungr, O., Evans, S.G., 1996. Rock avalanche runout prediction using a dynamic model. In: Proceedings of the Seventh International Symposium on Landslides, Trondheim, Nor-way, vol. 1, pp. 233–238.

Hungr, O., Evans, S.G., 2004. Entrainment of debris in rock avalanches; an analysis of a long run-out mechanism. Bulletin of the Geological Society of America 116, 1240–1252.

Hungr, O., Evans, S.G., Bovis, M., Hutchinson, J.N., 2001. Review of the classification of landslides of the flow type. Environmental and Engineering Geoscience VII, 221–238.

Hungr, O., Dawson, R., Kent, A., Campbell, D., Morgenstern, N.R., 2002. Rapid flow slides of coal mine waste in British Columbia, Canada. In: Evans, S.G., DeGraff, J.V. (Eds.), Catastrophic Landslides: Effects, Occurrence and Mechan-isms, vol. 15. Geological Society of America, Reviews in Engineering Geology, pp. 191–208.

Hungr, O., Corominas, J., Eberhardt, E., 2005. State of the Art Paper #4, Estimating landslide motion mechanism, travel distance and velocity. In: Hungr, O., Fell, R., Couture, R., Eberhardt, E. (Eds.), Landslide Risk Management. Proceed-ings, Vancouver Conference. Taylor and Francis Group, London, pp. 99–128.

Iverson, R.M., 1997. The physics of debris flows. Reviews of Geophysics 35, 245–296.

Iverson, R.M., Denlinger, R.P., 2001. Flow of variably fluidized granular masses across three-dimensional terrain, 1. Coulomb mixture theory. Journal of Geophysical Research 106, 537–552.

Iverson, R.M., Logan, M., Denlinger, R.P., 2004. Granular avalanches across irregular three-dimensional terrain: 2. Experimental tests. Journal of Geophysical Research 109, F01015.

Körner, H.J., 1976. Reichweite und Geschwindigkeit von Bergstürzen und Fließschneelawinen. (Reach and velocity of rockslides and powder snow avalanches). Rock Mechanics 8, 225–256.

Laigle, D., Coussot, P., 1997. Numerical modeling of mudflows. Journal of Hydraulic Engineering 123, 617–623.

Mangeney, A., Heirich, P., Roche, R., 2000. Analytical solution for testing debris avalanche numerical models. Pure and Applied Geophysics 157, 1081–1096.

Mangeney-Castelnau, A., Vilotte, J.P., Bristeau, O., Perthame, B., Bouchut, F., Simeoni, C., Yerneni, S., 2003. Numerical modeling of avalanches based on Saint Venant equations using a kinetic scheme. Journal of Geophysical Research 108 (B11), 2527.

Mangeney, A., Bouchut, F., Thomas, N., Vilotte, J.P., Bristeau, M.O., 2007a. Numerical modeling of self-channeling granular flows and of their levee-channel deposits. Journal of Geophysical Research 112, F02017.

Mangeney, A., Tsimring, L.S., Volfson, D., Aranson, I.S., Bouchut, F., 2007b. Avalanche mobility induced by the presence of an erodible bed and associated entrainment. Geophysical Research Letters 34, L22401.

McDougall, S., 2006. A New continuum dynamic model for the analysis of extremely rapid landslide motion across complex 3D terrain. Unpublished Ph.D. Dissertation, Department of Earth and Ocean Sciences, University of British Columbia, 253pp.

McDougall, S., Hungr, O., 2003. Objectives for the development of an integrated three-dimensional continuum model for the analysis of landslide runout. In: Rickenmann, D., Chen, C.L. (Eds.), Proceedings of the Third International Conference on Debris-Flow Hazards Mitigation: Mechanics, Prediction and Assessment, Davos. Millpress, Rotterdam, pp. 481–490.

McDougall, S., Hungr, O., 2004. A model for the analysis of rapid landslide motion across three-dimensional terrain. Canadian Geotechnical Journal 41, 1084–1097.

McDougall, S., Hungr, O., 2005. Dynamic modelling of entrainment in rapid landslides. Canadian Geotechnical Journal 42, 1437–1448.

O'Brien, J.S., Julien, P.Y., Fullerton, W.T., 1993. Two-dimensional water flood and mudflow simulation. Journal of Hydraulic Engineering 119, 244–261.

Pastor, M., Quecedo, M., Fernandez Merodo, J.A., Herrores, M.I., Gonzalez, E., Mira, P., 2002. Modelling tailings dams and mine waste dumps failures. Geotechnique 52, 579–591.

Perla, R., Cheng, T.T., McClung, D.M., 1980. A two-parameter model of snow-avalanche motion. Journal of Glaciology 26, 197–207.

Pudasaini, S.P., Hutter, K., 2007. Avalanche Dynamics. Springer, Berlin, Heidelberg, 602pp.

Revellino, P., Hungr, O., Guadagno, F.M., Evans, S.G., 2004. Velocity and runout simulation of destructive debris flows and debris avalanches in pyroclastic deposits, Campania region, Italy. Environmental Geology 45, 295–311.

Rickenmann, D., Koch, T., 1997. Comparison of debris flow modelling approaches. In: Chen, C.L. (Ed.), Proceedings of the 1st International Conference on Debris-flow Hazards Mitigation: Mechanics, Prediction and Assessment. American Society of Civil Engineers, New York, NY, pp. 576–585.

Sassa, K., 1985. The mechanism of debris flows. In: Proceedings of the 11th International Conference on Soil Mechanics and Foundation Engineering, San Francisco. International Society of Soil Mechanics and Foundation Engineering, vol. 1, pp. 1173–1176.

Savage, S.B., Hutter, K., 1989. The motion of a finite mass of granular material down a rough incline. Journal of Fluid Mechanics 199, 177–215.

Savage, S.B., Hutter, K., 1991. The dynamics of avalanches of granular materials from initiation to runout, Part 1: Analysis. Acta Mechanica 86, 201–223.

Sousa, J., Voight, B., 1991. Continuum simulation of flow failures. Géotechnique 41, 515–538.

Sovilla, B., Burlando, P., Bartelt, P., 2006. Field experiments and numerical modeling of mass entrainment in snow avalanches. Journal of Geophysical Research 111, F03007.

Stoker, J.J., 1957. Water Waves. Interscience, New York, NY, 250pp.

Takahashi, T., 1991. Debris Flow. International Association for Hydraulic Research monograph. A.A. Balkema, Rotterdam, 165pp.

Terzaghi, K., Peck, R.B., 1967. Soil Mechanics in Engineering Practice. Wiley, New York, NY, 729pp.

Voellmy, A., 1955. Über die Zerstörunskraft von Lawinen (On breaking force of avalanches). Schweizerische Bauzeitung 73, 212–285 (in German).

Voight, B., Pariseau, W.G., 1978. Rockslides and avalanches: an introduction. In: Voight, B. (Ed.), Rockslides and Avalanches, vol. 1. Elsevier, New York, NY, pp. 1–67.

Wang, Z., Shen, H.T., 1999. Lagrangian simulation of one-dimensional dam-break flow. Journal of Hydraulic Engineering 125, 1217–1220.